Physica C 212 (1993) 375–380
North-Holland

PHYSICA C

Hole spectrum of adjacent CuO_2 planes in the two-band model and the non-monotonic T_c dependence on the external parameters

A.F. Barabanov
Vereschagin Institute for High Pressure Physics, 142092, Troitsk, Moscow Region, Russian Federation

L.A. Maksimov and L.E. Zhukov
Kurchatov Institute, 123182, Moscow, Russian Federation

Received 18 December 1992
Revised manuscript received 18 april 1993

The single hole spectrum $\epsilon(k)$ of adjacent CuO_2 planes is studied within a framework of a two-band model for small-radius magnetic polaron. The Fermi level position relative to the magnetic Brillouin zone boundary depends strongly on the value of the interplane hole hopping parameter h and the hole concentration x at small x. Within this approach a qualitative explanation of the non-monotonic T_c behaviour as a function of concentration, pressure and number of adjacent CuO_2 layers in HTSC is given.

1. Introduction

It is well known that the temperature T_c of the superconductive transition for the high-temperature $La_{2-x}Sr_xCuO_4$ superconductor depends non-monotonically on the hole concentration x [1]. A similar behaviour of T_c as a function of x is observed in Y- and Tl-based superconductors, such as $YBa_2Cu_3O_{7-\delta}$ and $TlSr_2(Er_{1-2x}Sr_{2x})Cu_2O_{2x-\delta}$ [2]. In addition, the pressure dependence of T_c shows a monotonic T_c increase for HTSC with low carrier concentration in the Y 1–2–3 and Tl 1–2–1–2 systems and non-monotonic behaviour with a maximum in the $T_c(P)$ curve for samples with a high carrier concentration [3]. It is also found that in $Tl_2Ba_2Ca_{n-1}Cu_nO_{2n+4}$ compounds the transition temperature T_c has a maximum as a function of n, where n is the number of adjacent layers in a unit cell [4].

In the present paper we propose a qualitative explanation for such T_c behaviour which is based on specific features of the hole spectrum E_k in a framework of the magnetic polaron approach. In order to describe the hole motion in a single CuO_2 plane we start with the two-band Hubbard model [5]. We also assume the possibility of interplane hole hopping via the neighboring O sites belonging to the adjacent CuO_2 planes. The spectrum E_k will be obtained by using the variational method for hole wave functions. As has been shown in ref. [6] for the case of the Néel spin state of the Cu subsystem with the realistic value of parameter $J \cong 0.25\tau$, where J is the constant of AFM Cu–Cu exchange coupling and τ is the effective hole hopping parameter, the excitation spectrum can be described correctly in the framework of the theory of a magnetic polaron of small radius. The hole spectrum depends essentially on the behaviour of spin correlation functions in the Cu sublattice. We consider the singlet ground state $|G\rangle$ of the spin subsystem of the CuO_2 plane as the RVB state, i.e. we assume that the spin correlation functions $\langle S^{\alpha}_{R1} S^{\beta}_{R2} \rangle$ have AFM character but possess spherical symmetry, and the average Cu-site spin projection $\langle S^{\alpha}_{R} \rangle = 0$, $\alpha = x, y, z$; $\langle ... \rangle \equiv \langle G | ... | G \rangle$ [7]. In the case of small doping our description results in the spectrum ϵ_k which has large parts of the Fermi surface near the magnetic Brillouin zone boundary, defined by the equation $\gamma_k = (\cos(k_x 2a) + \cos(k_y 2a))/2 = 0$, where a is the distance between Cu and O nearest-neighboring (NN) sites in a CuO_2 plane (see fig. 1).

As is shown in ref. [8], the existence of the Fermi surface sheets close to the corners X of the magnetic

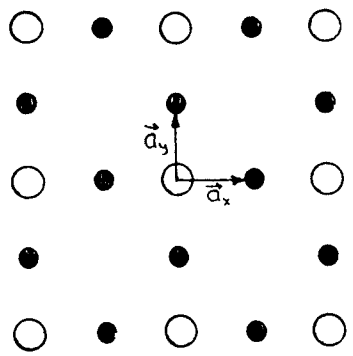

Fig. 1. The structure of the CuO_2 plane: O – Cu sites, ● – O sites, a_x and a_y are the O-site vectors in the unit cell.

Brillouin zone $\gamma_k=0$ (see fig. 2(a)) is very important for the problem of superconductivity because it results in a large density of states on the Fermi surface near the Van Hove singularities. Superconductivity arises owing to the nesting near X points which stimulates strong anisotropy of the pairing interaction. However, the superconductive state becomes unstable with respect to the spin-density wave formation, when the sheet of energy ϵ_F reaches the line $\gamma_k=0$. This result gives the background for our main qualitative assumption: the maximum value of T_c occurs when the Fermi surface reaches some optimal surface of equal energy near the line $\gamma_k=0$.

The paper is organized as follows. In section 2 we introduce the effective hamiltonian and describe the method and results of E_k calculations. Section 3 contains the discussion of the results and interpretation of the experimental dependence of T_c on concentration x, pressure P and the number of adjacent CuO_2 planes n.

2. Model and method of spectrum calculations

We start with the effective hamiltonian for an extra hole in two CuO_2 layers which is the simplest generalization of the well-known two-band-one-layer hamiltonian [5],

$$\hat{H}=\hat{T}+\hat{h}\,, \tag{1}$$

$$\hat{T}=\sum_{i}\sum_{\substack{R,a_1,a_2\\ \sigma_1,\sigma_2}}[\tau(1-\delta_{a_1,a_2})+\tau_1\delta_{a_1,a_2}\delta_{\sigma_1,-\sigma_2}]$$

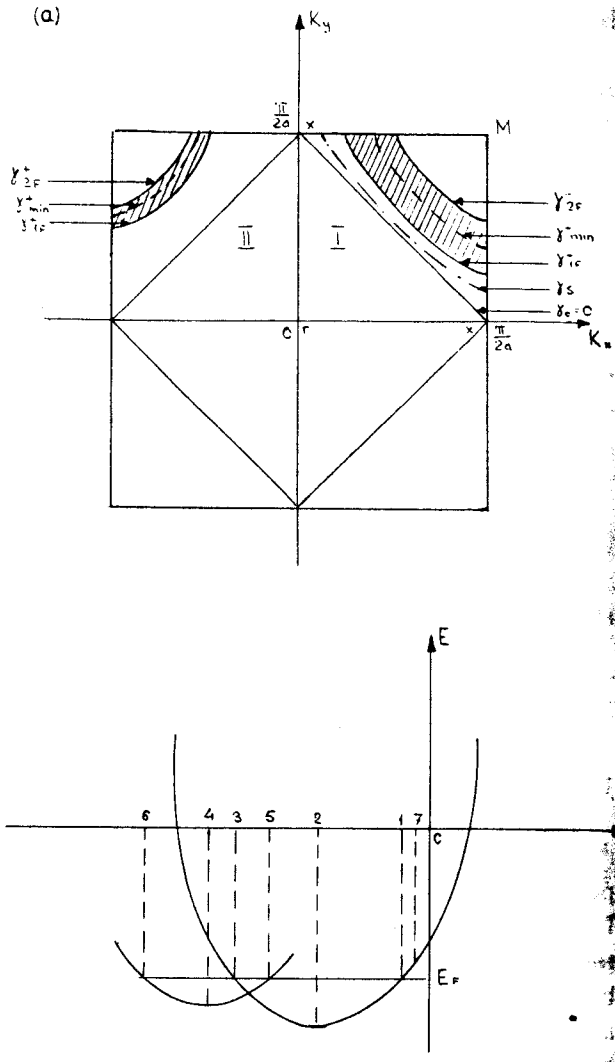

Fig. 2. (a) The full and the reduced magnetic Brillouin zone for the CuO_2 plane. The equal energy lines for E_k^- and $E_k^+=\text{const}$ are represented schematically in the first and the second quadrant, respectively. The dashed line represents the bottoms of two bands, lines $\gamma_{min}^{\pm}$; the solid line represents the lines of the Fermi surface γ_{1F}^-, γ_{2F}^-, γ_{1F}^+, γ_{2F}^+; the dash–dotted line represents the equal energy line γ_s which determines the optimal condition for T_c. (b) The schematic dependence of the energies of two bands E^- and E^+ on $\gamma=(\cos(2ak_x)+\cos(2ak_y))/2$. The points 1–7 represent the corresponding lines γ_{1F}^-, γ_{min}^-, γ_{2F}^-, γ_{min}^+, γ_{1F}^+, γ_{2F}^+, γ_s in fig. 2(a). The doping level determines the chemical potential E_F.

$$\times Z_{i,R}^{\sigma_1\sigma_2}C_{i,R+a_2,\sigma_2}^{+}C_{i,R+a_1,\sigma_1}\,,$$

$$\hat{h}=h\sum_{r}(C_{1,r,\sigma}^{+}C_{2,r,\sigma}+\text{h.c.})\,,$$

$$i=1,2;\quad a_1,a_2=\pm a_x,\ \pm a_y;$$

$$\tau=t^2/\epsilon;\quad \tau_1=t^2/(\epsilon+U_p)\,;$$

Here and below $r=R+a$ are four vectors of O sites nearest to the Cu site R; the operator C_σ^+ creates a hole with a spin index $\sigma=\pm1$ at the O site and $\hat{f}_{i,R}^{\sigma\sigma}$ is the Hubbard projection operator which is introduced to exclude the doubly occupied states of Cu sites; $i=1, 2$ stands for the number of CuO_2 planes.

The first term $\hat{T}$ in eq. (1) describes the effective hole hopping from O to O sites through the intervening Cu sites. It can be obtained within the perturbation theory in $t/\epsilon \ll 1$ from the site hamiltonian which is characterized by the Cu and O hole levels ϵ_d and ϵ_p ($\epsilon=\epsilon_p-\epsilon_d>0$), the NN Cu–O hopping t, and the intrasite Hubbard repulsion energies U_d and U_p, respectively [9].

We take $U_d=\infty$ as the largest energy parameter. The $\sigma_1\neq\sigma_2$ hopping terms in $\hat{T}$ describe a simultaneous spin flip of Cu and O holes.

The second term $\hat{h}$ in eq. (1) describes the hole hopping between NN O-sites from different CuO_2 planes. The planes under consideration have Cu (O) sites one above the other.

We assume for the Hubbard model parameters the inequality $h<\tau$, and take $U_p=0$ because the results are found to depend weakly on the value of this parameter.

The hole excitation in the two-band Hubbard model is known to form a magnetic polaron [5,10]. As we consider the hole excitation spectrum $E(k)$ in the approximation of a magnetic polaron of small radius, the set of the site functions $\varphi_{i,R}$ is close to the Zhang–Rice singlet [10]. The trial Bloch wave function Ψ should contain explicitly the wave function $|G\rangle$ of the Cu spin subsystem. For $\sigma=+1$ the function Ψ_k can be written as

$$\Psi_k=\sum_{i,R}\lambda_i e^{ikR}\varphi_{i,R}\,,\quad \varphi_{i,R}=\hat{\varphi}_{i,R}^+|G\rangle\,, \tag{2}$$

$$\hat{\varphi}_{i,R}^+=\tfrac{1}{2}\sum_{a=\pm a_x,\pm a_x}(C_{i,R+a,+1}^+Z_{i,R}^{--}-C_{i,R+a,-1}^+Z_{i,R}^{+-})\,.$$

We assume that state $|G\rangle$ of the Cu two-layer subsystem is the singlet [7]. Using the singlet character of the state $|G\rangle$ it is easy to find that $\hat{S}_{tot}^z\varphi_{i,R}=\frac{1}{2}\varphi_{i,R}$ and $\hat{S}_{tot}^2\varphi_{i,R}=\frac{3}{4}\varphi_{i,R}$, where $\hat{S}_{tot}$ is the spin operator of the total system. The polaron spectrum $E(k)$ is obtained by the variational method with λ_i as a variational parameter. In the two-layer model we have, obviously, $\lambda_1=\pm\lambda_2=\pm2^{-1/2}$.

The element of the secular matrix $E(k)$ contains two- and three-site Z-operator correlation functions. Owing to the singlet nature of the ground state $|G\rangle$ the matrix elements can be expressed in terms of the pair spin correlations. For example, $\langle Z_{1,R+2a_1}^{+-}Z_{1,R}^{++}Z_{1,R+2a_2}^{-+}\rangle=\frac{1}{3}\langle S_{1,R+2a_1}S_{1,R+2a_2}\rangle=\frac{1}{3}C_2$. As in ref. [7], we also assume that in one layer the pair site correlations between the second and the third NN Cu spins coincide.

The explicit calculations lead to the following expressions for two bands:

$$E_k^\pm=\epsilon_k\pm h_k\,;\quad \epsilon_k=-4\tau-\tau\frac{4A\gamma_k-B(\gamma_k^2-\frac{1}{4})}{1+A\gamma_k}\,;$$

$$h_k=h\frac{|A_1'+A_2'\gamma_k|}{1+A\gamma_k}\,, \tag{3}$$

where

$$A=\tfrac{1}{4}+C_1\,,\quad C_1=\langle S_{1,R}S_{1,R+2a}\rangle\,;$$

$$B=4(\tfrac{1}{8}+C_2/2-C_1)\,;\quad C_2=\langle S_{1,R}S_{1,R+2a_1+2a_2}\rangle\,;$$

$$A_1'=\tfrac{1}{4}+C_1'\,;\quad C_1'=\langle S_{1,R}S_{2,R}\rangle\,;$$

$$A_2'=\tfrac{1}{4}+C_2'\,;\quad C_2'=\langle S_{1,R}S_{2,R+2a}\rangle\,;$$

$$\gamma_k=(\cos(2ak_x)+\cos(2ak_y))/2\,; \tag{4}$$

For the undoped dielectric single-layer case which is described usually by the Heisenberg model, different approaches lead to similar values for the state correlations $C_1=-0.351$; $C_2=0.213$ [7]. Then $A=-0.101$ and $B=2.33$. We use these values in numerical calculations. The exchange interaction between adjacent layers is considerably less in comparison with the Cu–Cu intralayer interaction. That is why we take [11]:

$$C_1'=0.1\,C_1\,;\quad C_2'=0.1\,C_2\,. \tag{5}$$

As concerns the parameter h in eq. (1), we represent numerical results corresponding to $\alpha=h/\tau=0.01$.

The E_k expression for two layers can be easily generalized for three- and four-layer cases:

$$E_k=\epsilon_k,\ \epsilon_k\pm\sqrt{2}h_k,\ \text{for three layers}\,;$$

$$E_k=\epsilon_k\pm((3\pm\sqrt{5})/2)^{1/2}h_k,\ \text{for four layers}\,; \tag{6}$$

where ϵ_k and h_k are the same as in eq. (3).

3. Results and discussion

The lines $\gamma_k = \text{const}$ are the lines of equal energy for the upper E_k^+ and lower E_k^- bands of the spectrum (3). We introduce the notation $\gamma_{\min}^{\pm}$ for the lines corresponding to the $E_k^{\pm}$ band bottoms. These lines and the spectrum $E^{\pm}(\gamma)$ are shown schematically in fig. 2(a). The important property of the $E_k^{\pm}$ spectrum is the location of the $\gamma_{\min}^-$ line close to the magnetic Brillouin zone boundary $\gamma_k = \gamma_0 = 0$. This is the consequence of the $|G\rangle$ state correlation functions which give $|A| \ll |B|$. This result seems to be an important property of the model. The constants A and B describe the magnetic polaron hopping between the first and the second NN sites, respectively. Owing to strong short-range AFM correlations the magnetic polaron moves mainly over one of the Cu magnetic sublattices, though there are no real sublattices in Cu subsystem state $|G\rangle$. For the case of the Néel state G_N we have a similar situation, $|A| = \frac{1}{4} - \langle S_R S_{R+a}\rangle = 0 \ll B$. However, for the Néel state the spectrum $E_k^{\pm}$ must be symmetric with respect to the magnetic zone boundary, unlike the case of a singlet $|G\rangle$. For the chosen values of C_i'/C_i (5) the line $\gamma_{\min}^+$ is always shifted to the point M relative to the position of the line $\gamma_{\min}^-$ (see fig. 2(a)). This shift depends on the parameter $\alpha = h/\tau$ and increases with the increase of α.

We represent our numerical results for the sufficiently small value of parameter $\alpha = 0.01$ (small values of α correspond to the most interesting case of the two-band filling). Figure 3 demonstrates the equal energy lines for E_k^-. The $\gamma_{\min}^-$ is shown by the dashed line with the energy $E_{\min}^- = -4.597$; hereafter we put $\tau = 1$. All other lines of equal energy on both sides of $\gamma_{\min}^-$ correspond to the values E_k^- with the step $\Delta E = 0.03$. The lines for the second band E_k^+ have the same form but these lines are shifted to the point M. The characteristic spectrum E_k^- along the principal axes of the Brillouin zone is given in fig. 4.

The inset to fig. 5 represents the density of states $\rho(E)$ for both bands in a wide energy range. In fact, the peak of the density of states has the fine structure due to the Van Hove singularities near the bottoms of two bands (square root singularities $|\gamma - \gamma_{\min}^+|^{-1/2}$ and $|\gamma - \gamma_{\min}^-|^{-1/2}$) and near the corners X of the magnetic Brillouin zone (saddle points with the logarithmic singularities). These singularities of

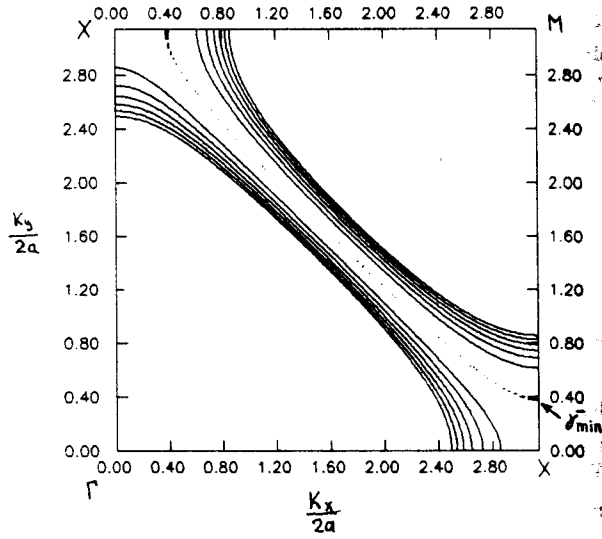

Fig. 3. Equal energy lines $E_k^- = \text{const}$ for $\Delta E = 0.03$; $\alpha = h/\tau = 0.01$. The dashed line $\gamma_{\min}^-$ is the bottom of the lower band E_k^-.

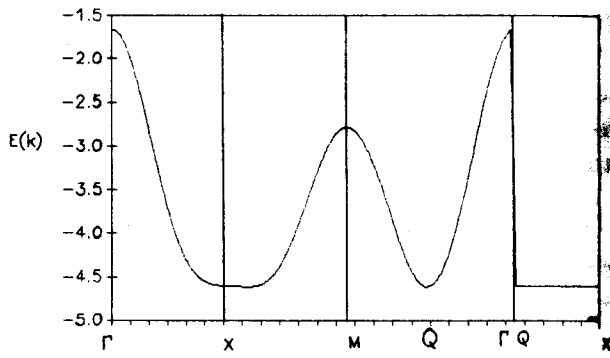

Fig. 4. The lower band E_k^- spectrum along the principal axes for $\alpha = 0.01$ and $\tau = 1$.

$\rho(E)$ are shown in fig. 5. The peaks for $E^-(\gamma_{\min}^-) = -4.597$ and $E^+(\gamma_{\min}^+) = -4.593$ correspond to the bottoms of two bands. The third peak $E^-(\gamma_0) = -4.584$ and the fourth peak $E^+(\gamma_0) = -4.581$ correspond to the X corners.

As α increases, the $\rho(E)$ peaks $E^-(\gamma_{\min}^-)$ and $E^-(\gamma_0)$ are seen to be shifted to the left and the peaks $E^+(\gamma_{\min}^+)$ and $E^+(\gamma_0)$ are shifted to the right relative to their position in fig. 5. For $\alpha \geq 0.03$ the peak of the E_k^+ band bottom crosses the position of the right $E_k^-(\gamma_0)$ peak.

As to the Fermi surface, there can be two different situations depending on the values of the parameter $\alpha = h/\tau$ and the hole concentration x. Hereafter x is

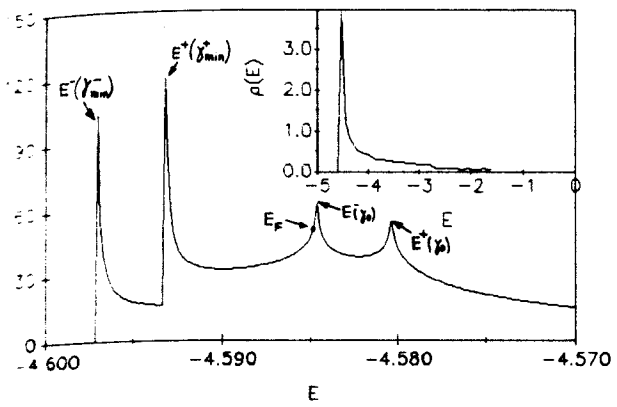

Fig. 5. The fine structure for the bottom spectrum peak of the density of states $\rho(E)$. The position E_F corresponds to $x \sim 0.24$. Four subpeaks $E^-(\gamma^-_{min})$, $E^+(\gamma^+_{min})$, $E^+(\gamma_0)$, $E^-(\gamma_0)$ correspond to the Van Hove singularities. Here $\tau=1$, $\alpha=0.01$. The inset represents $\rho(E)$ for the two bands $E^{\pm}_k$ in a wide range of energy.

the number of holes per Cu atom in the CuO_2 plane. For small x or sufficiently large α the E^+_k band is empty and the Fermi surface consists of two sheets corresponding to the γ^-_{1F} and γ^-_{2F} lines, $\gamma^-_{1F} > \gamma^-_{2F}$ (see figs. 2(a) and (b)). For sufficiently large x or rather small $\alpha < 0.03$, the holes fill the E^+_k band and two additional Fermi sheets, γ^+_{1F}, γ^+_{2F}, appear (figs. 2(a) and (b)).

We discuss below the case of two partially filled bands. From the point of view of the phase transitions the most interesting situation takes place when one of the Fermi sheets γ^-_{1F} or γ^+_{1F} lies close to the line γ_0. In this case, a detailed analysis of the superconducting properties in the weak coupling approximation was given in ref. [12]. As can be seen from fig. 2(b) in our model with $x=0.24$ and $\alpha=0.01$, the sheet γ^-_{1F} is the closest to γ_0 and, therefore, this sheet is responsible for possible instabilities in this system.

The proximity of γ^-_{1F} to γ_0 was used in ref. [8]. It was shown that in this case the interaction between the small radius polarons could result in a superconducting state with d- or s-pairing. The superconducting state arises owing to the strong anisotropy of the pairing interaction. The main condition for superconductivity is determined by two inequalities for the γ^-_{1F} equienergy line [8]:

$$(2\pi)^{-1}(U_{\text{eff}}/\tau)\ln(1/\gamma^-_{1F}) < 1; \quad \ln(1/\gamma^-_{1F}) \gg 1; \quad (7)$$

where U_{eff} is the constant of effective interaction between magnetic polarons. These inequalities permit one to formulate a qualitative criterion of the optimum conditions for superconductivity. The highest value of the transition temperature T_c occurs when the γ^-_{1F} sheet of the Fermi surface coincides with some optimum line $\gamma_k = \gamma_s$, which lies close to the line γ_0 (see figs. 2(a) and (b)). In our analysis we put $\gamma_s = -0.042$, and the corresponding energy equals $E^-_k(\gamma_s) = -4.586$ at $\alpha = 0.01$. As the hole concentration x increases the sheet γ^-_{1F} moves from the bottom line γ^-_{min} to the line γ_s. We denote by x_s the hole concentration for which sheet γ^-_{1F} crosses the line γ_s. The calculation gives $x_s = 0.24$. So, in the framework of our criterion the transition temperature T_c as a function of the hole concentration x increases up to $x_s = 0.24$ and for larger doping $x > x_s$ the transition temperature decreases.

Now we discuss the influence of changing the parameter α or h on the position of γ^-_{1F} with respect to the line γ_s. For fixed and small x the increase of parameter α results in a shift of γ^-_{min} and consequently γ^-_{1F} towards the line γ_0. If x is sufficiently small, the sheet $\gamma^-_{1F}(x_0, \alpha)$ lies far enough from γ_s, and the sheet γ^-_{1F} does not cross γ_s at any α. This means that T_c is a monotonic function of α. But, for the case of large doping ($x \geq 0.2$), the same α increase is enough for γ^-_F and γ_s to cross. This situation corresponds to the passage of the superconductive transition temperature through the maximum.

The dependence of the lattice constants and bond lengths on hydrostatic pressure for 1-2-3 HTSC compounds [13] indicates that the interplane compressibility is smaller than the intraplane one. This means that the effect of hydrostatic pressure should lead to increasing parameter α.

So, we obtain that the experimental T_c dependence on the hole concentration $x \cong (0.5-\delta)/2$ and pressure P for $YBa_2Cu_3O_{7-\delta}$ should be qualitatively described by the following expression:

$$T_c = \beta_0 - \beta_1(\gamma^-_F(x, \alpha) - \gamma_s)^2, \quad (8)$$

where β_0 and $\beta_1 > 0$ are the fitting parameters. In particular, we suppose that zero pressure corresponds to $\alpha = 0.005$, and the concentrations $x = 0.03$ and $x = 0.2$ lead to the critical temperatures $T_c = 62$ K and $T_c = 90$

K, respectively. Then we obtain the coefficients: $\beta_0=91$ and $\beta_1=4.4\times10^4$. The resulting dependence of critical temperature T_c on the parameter α is shown in fig. 6 together with the experimental data $T_c(P)$ for compounds $YBa_2Cu_3O_{7-\delta}$ with $\delta=0.1$ and $\delta=0.45$ [14]. As can be easily seen, the experimental results qualitatively coincide with the calculated T_c dependence.

For Tl-based compounds the critical temperature T_c dependence on n, the number of adjacent CuO_2 layers in a unit cell, has a maximum at $n=4$ [4]. It follows from eq. (5) that increasing n at fixed hole concentration x results effectively in the enhancement of parameter h and, thus, α. For the typical values $x=0.2$ and $\alpha=0.01$ we obtain a similar dependence $T_c(n)$ as in ref. [4].

In the framework of our main approximations, i.e. small polaron radius and T_c maximum criterion based on the inequalities (7), the above-discussed T_c behaviour as a function of x, α and n holds true in a wide range of the parameters involved. The values $\alpha>0.03$ result only in the lower band filling for $x\sim0.25$. As a result the Fermi line $\gamma_{\bar{1}F}$ crosses γ_s at a lower concentration of holes and T_c maximum occurs at $x_s<0.24$. The increase of the relation C_i'/C_i leads to the increase of x_s.

These results are still valid if we extend the set of the chosen trial site functions $\varphi_{i,R}$ (2) by involving the additional functions $C^+_{i,R+a_x,+1}|G\rangle$ and $C^+_{i,R+a_y,+1}|G\rangle$.

In conclusion, we note that it is commonly accepted that the superconductivity in $YBa_2Cu_3O_{7-\delta}$ and YBa_2CuO_8 depends on charge transfer phenomena [15]. The displacement of the apical oxygen atoms to the CuO_2 planes under pressure is associated with the hole transfer from the chains to the CuO_2 planes, i.e. with the increase of concentration x. The pressure-induced changes of T_c based on the charge transfer assumption do not contradict our theory. The additional x increase changes the relative $\gamma_{\bar{1}F}$ and γ_s position in the same way as the parameter h does. Thus, we can take into account the x-transfer simply by rescaling the parameter h dependence on pressure.

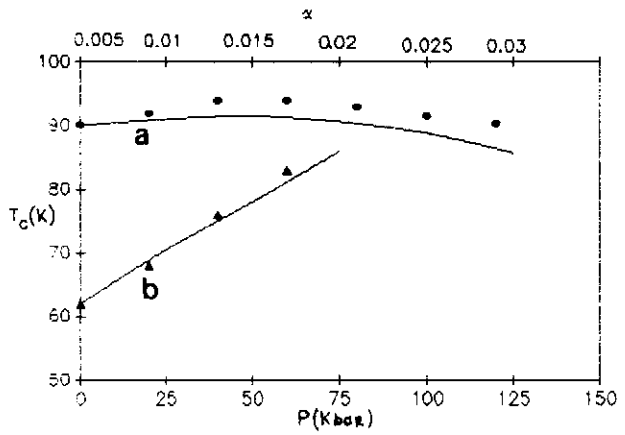

Fig. 6. The T_c dependence on α in the approximation: $T_c=\beta_0-\beta_1(\gamma_{\bar{F}}(x,\alpha)-\gamma_s)^2$, $\alpha=0.01$ and (a) $x=0.2$, (b) $x=0.03$. The experimental points of T_c dependence on P are taken from ref. [15] for the superconductors $YBa_2Cu_3O_{7-\delta}$ with: ● – $\delta=0.1$, ▲ – $\delta=0.44$.

References

[1] R.M. Fleming et al., Phys. Rev. B 35 (1987) 7191; Y. Kitaoka et al., Physica C 153–155 (1988) 153.
[2] D.C. Johnston et al., Physica C 153–155 (1988) 572.
[3] N. Mori and C. Murayama, Physica C 185–189 (1991) 40; N.E. Monlton and S.A. Wolf, Phys. Rev. B 44 (1991) 12632.
[4] H. Ihara et al., Bull. Electrotech. Lab. 53 (1989) 57; S. Nakajima et al., Physica C 158 (1989) 471.
[5] V.J. Emery and G. Reiter, Phys. Rev. B 39 (1988) 4547; A.F. Barabanov, L.A. Maksimov and G.V. Uimin, Sov. Phys. JETP 69 (1989) 371.
[6] A.F. Barabanov, R.O. Kuzian, L.A. Maksimov and G.V. Uimin, Supercond.: Phys. Chem. Technol. 3 (1990) 8; Progress in HTSC, eds. V.L. Aksenov et al., Vol.21 (1989) p.477.
[7] J. Oitmaa and D. Betts, Can. J. Phys. 56 (1978) 897D; Doucot, S. Liang and P.W. Anderson, Phys. Rev. Lett. 61 (1988) 365; A.F. Barabanov, O.A. Starykh and L.A. Maksimov, Int. J. Mod. Phys. B 4 (1990) 2319.
[8] A.N. Kozlov, L.A. Maksimov and A.F. Barabanov, Physica C 200 (1992) 183.
[9] F. Mila, Phys. Rev. B 38 (1988) 11358; M.S. Hybersten and M. Schulter, Phys. Rev. B 39 (1989) 9028.
[10] F.C. Zhang and T.M. Rice, Phys. Rev. B 37 (1988) 3759.
[11] K. Hida, J. Phys. Soc. Jpn. 59 (1990) 2230.
[12] I.E. Dzyaloshinskii and V.M. Yakovenko, Sov. Phys. JETP 94 (1988) 344.
[13] H. Takahashi et al., Jpn. J. Appl. Phys. 26 (1987) 4504.
[14] M.A. Ilyina, Supercond.: Phys. Chem. Technol. 4 (1991) 726; Lotter, Wittiy, Physica C 153–155 (1988) 1353.
[15] J.D. Jorgensen et al., Physica C 171 (1990) 93; Y. Yamada et al., Physica C 173 (1991) 185.